NOVEL COMPOSITE BASED ON ZIRCONIA AND GRAPHITE. FIRST RESULTS OF APPLICATION FOR SYNTHETIC DYES REMOVAL

**KATARINA STEPIĆ[a], RADOMIR LJUPKOVIĆ[a,*],
ALEKSANDRA ZARUBICA[a], STEFAN ĐORĐIJEVSKI [b],
BRANKO MATOVIĆ[c], JUGOSLAV KRSTIĆ[d],
ALEKSANDAR BOJIĆ[a]**

ABSTRACT. In this research composite based on zirconia and graphite was synthesized using the sol-gel method. Aim of this research is to activate and increase the photocatalytic activity of ZrO_2 by combining with graphite-based material. Our results show that we obtained material that can remove both cationic and anionic dyes by sorption and photocatalytic processes. Obtained composite is very effective in sorption of RB19 with up to 100% removal. Photocatalytic activity of composite is higher than pristine GO and goes up to 100% for RB19 degradation and about 50% degradation of MB. These results are promising and present an excellent base for further research.

Keywords: *Composite, Zirconia, Graphite, Methylene blue, Reactive blue 19, Sorption, Photocatalysis, UV degradation*

INTRODUCTION

The dyes and their intermediates are the second most dangerous water pollutant, immediately after agriculture, and dye contamination of water is a major global problem that caused severe issues for nature and human society [1]. They are easy to recognize in the water, even at very low concentrations (aesthetically undesirable and easily soluble), and some dyes and their degradation products may be toxic and carcinogens, which is why

[a] *Department of Chemistry, Faculty of Science and Mathematics, University of Niš, Višegradska 33, Niš 18000, Serbia.*
[b] *Mining and Metallurgy Institute, Bor, Zeleni bulvar, Serbia.*
[c] *Institute for Nuclear Sciences Vinča, University of Belgrade, Belgrade 11351, Serbia.*
[d] *Institute of Chemistry, Technology and Metallurgy, University of Belgrade, Njegoševa 11, 11000 Belgrade, Serbia.*
[*] *Corresponding author: radomir.ljupkovic@pmf.edu.rs, ljupkovic@gmail.com.*

they are very harmful to the aquatic world [2]. Some of the dyes mentioned in this paper are Methylene blue (MB) and Reactive blue 19 (RB 19). Methylene blue is an organic salt (methylthioninium chloride) that has wide application in the cotton, silk, paper and wood industry. This dye can have various harmful effects, although it is not strongly dangerous, it can induce eye burns which may be responsible for permanent injury to the eyes of humans and animals [3]. Also, it can cause short periods of rapid or difficult breathing if inhaled [4]. Reactive blue 19 is an anthraquinone dye and is most commonly used in the textile industry because of its high color stability and low degradability [5]. RB 19 is very toxic for aquatic organisms and unsuitable for human health [6]. The main difference between these two dyes is that RB 19 contains two anionic sulfonate groups on its structure which renders a negative charge to it, while MB has a positive charge because of cationic groups on its structure.

Methods such as adsorption [7], biodegradation [8], oxidation [9], photocatalytic degradation [10] and ultrafiltration [11] have been used for the removal of dye pollutants from wastewater. Among all these processes, sorption is considered a conventional, but efficient, easy and economic process. Adsorption is an effective method for water decolorization that does not result in the formation of hazardous substances [12]. Many materials (commercial active carbon, bioadsorbents, natural materials and wastes from agriculture) have been used for adsorption processes and the choice depends on the properties of the required adsorbent [13].

Photocatalytic reactions are known as a sustainable method of the removal of many environmental pollutants in which we use photocatalysts to initiate reactions decomposition of contaminants under ultraviolet (UV) or sunlight irradiation without using chemical substances or producing chemical wastes. Today, UV water purification is one of the most effective method for water treatment with an efficiency greater than 99%. Photocatalytic treatments are also cheap and eco-friendly methods for water purification, where the main limiting factors are wide band gap and fast electron/hole recombination of used photocatalyst [14]. The surface properties of photocatalytic material have been modified to improve photocatalytic activity. Various heterogeneous semiconductors (TiO_2, ZnO, SnO_2, ZrO_2) are most commonly used for this purpose [15].

Nowadays, graphene and its derivates are used in environmental applications for the removal of different pollutants from wastewater. Graphene oxide (GO) is a layered solid compound with a large number of oxygen-containing functional groups that are known to stabilize the colloidal form of GO material [16]. A useful discovery is that graphene oxide can be directly used as an effective absorbent for the decoloration of methylene blue. The main advantages of GO usage for the removal of MB are high absorption capacity for MB and a fast adsorption process [7]. There are methods of

synthesis of GO which can be divided into bottom-up methods where carbon molecules build pristine graphene, and "top-down" methods where layers of graphene derivatives are obtained from a carbon source, such as graphite [17,18]. Bottom-up synthesis covers chemical vapor deposition, epitaxial growth, etc. are time consuming [19]. Graphene oxide can be prepared by the conventional and modified Hummers-Offeman method [20], whose principle is the oxidation of graphite with strong oxidizing agents to exfoliate graphite. GO coatings can also been made on various supports. L.C. Pop et al. deposited GO on a polypropylene membrane by the patented process. GO suspension was obtained by the oxidative-exfoliation method by using a mixture of sulphuric and phosphorous acid in combination with $KMnO_4$, followed with H_2O_2 adding and washing with water, hydrochloric acid and ethanol [21].

It has been reported that doping of graphene oxide based materials with a variety of heterogeneous semiconductors results in surface modification and significant improvement in its adsorptive and photocatalytic properties. As example, Wang et al. synthesized g-C_3N_4/CeO_2/N-rGO heterocomposite which exhibits enhanced photocatalytic activity in compare to pristine g-C_3N_4, CeO_2 nanorods [22]. Chauhan et al. found that GO/ZnO photocatalyst constantly developed over silicon substrate have 33% higher photodegradation of MB dye compared to pristine ZnO [23]. ZrO_2 is a widely used catalyst in photocatalyst reaction, mainly because of its favorable textural, structural, morphological and surface properties. Zirconium oxide is chemically inert, non-toxic, and insoluble in water, and because of these features, it is great dopant material [24].

The application of zirconia-graphene oxide based composites is explained in this paper, as one of the effective doped photocatalysts for the removal of organic dyes from water. It is presented an economical and eco-friendly method for obtaining ZrO_2-graphene oxide based composite by using a modified sol-gel method, and also the influence of zirconium-doping on physical and chemical properties and activity of graphene oxide. Decolorization of cationic dye MB and anionic dye RB 19 was used as a test reaction for examination of the activity of sorbents, while degradation of the above mentioned dyes under UV light irradiation was used as a test reaction for examination of the activity of catalysts.

RESULTS AND DISCUSSION

Characterization of synthesized materials

FT-IR spectrum of pure GO contains broad band with a maximum at 3442.47 cm^{-1} which can be assigned to vibrations of water molecules and O-H bonds. Most of the other present peaks can be assigned to C=C, and C-O

vibrations, with exception of the band at 645.10 cm^{-1} which represent O-H bending vibrations. At 1100.72 cm^{-1} is a peak that represents C-O-C vibrations [25]. The peak at 1212.85 cm^{-1} can be assigned either to C-O vibrations or vibrations that originate from covalent sulfates. Different C=C vibrations are represented by peaks at 1563.10, 1583.34, and 1630.11 cm^{-1}, while C=O can be described by peak at 1718.83 cm^{-1} [26]. All these peaks are represented in the following Figure 1.
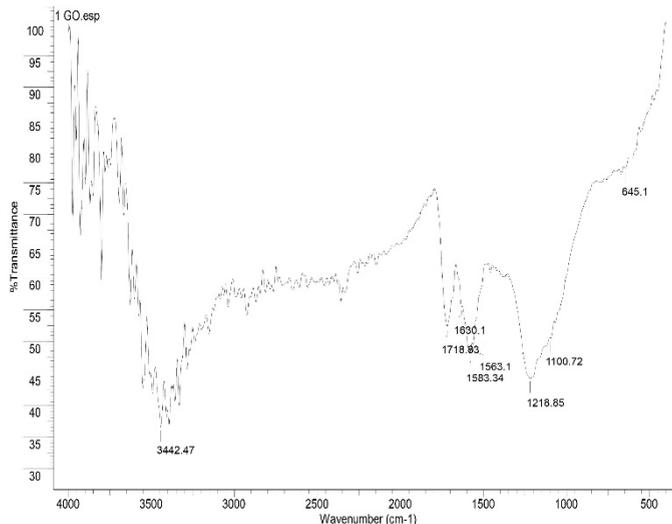

Figure 1. FT-IR spectrum of GO sample.
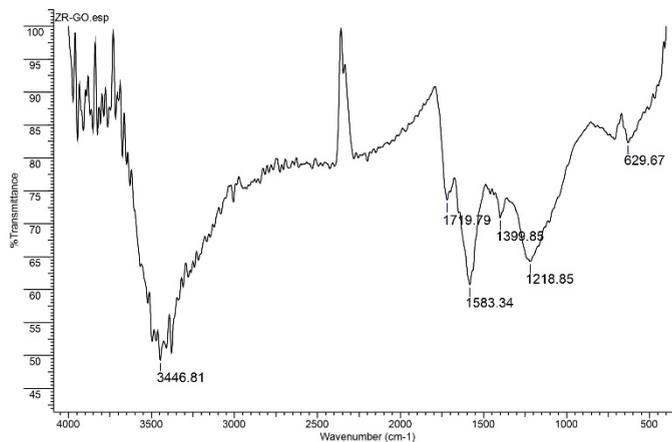
Figure 2. FT-IR spectrum of composite ZrO$_2$/GO.

In FT-IR spectra of ZrO_2/GO loss of bands for C-O-C (1100.72 cm^{-1}) and C=C (1563.10 and 1630.11 cm^{-1}) is observed. The band at 629.67 cm^{-1} can be assigned to Zr-O vibrations. The peak at 1399.65 cm^{-1} can be originated from Zr-OH vibrations. Other present vibrations are assigned to common graphite/graphene oxide vibrations: 1218.85 cm^{-1} for C-O, 1583.34 cm^{-1} for C=C stretching, 1718.83 cm^{-1} for C=O, and 3442.47 cm^{-1} for water [24]. All these peaks assigned to composite ZrO_2/GO are represented in the following Figure 2.

Diffractograms of our samples show relatively low crystallinity. The diffractogram of the GO sample shows a dominant wide peak at 2θ 26° which is a reflection of graphite planes [24]. Also, there are peaks at 2θ 43° and 2θ 13° as reflections correspond to (001) and (100) planes of GO [27]. We can assume that the oxidation of graphite was incomplete, so we have reflection corresponding to graphite and GO planes. All these peaks assigned to the GO sample are represented in the following Figure 3.
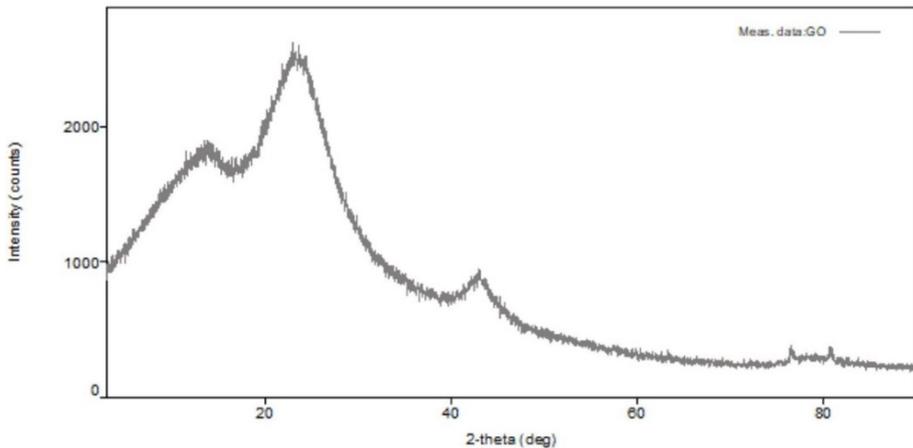
Figure 3. XRD diffractogram of GO sample.

Diffractogram of ZrO_2/GO shows a similar pattern, but the peak at 2θ 13° has been moved to lower angles, near to 2θ 5°. There are no reflections of ZrO_2 which can be explained by the low content of ZrO_2 in the sample and the absence of thermal treatment which is required to create crystalline ZrO_2 phases. All peaks assigned to composite ZrO_2/GO are represented in the following Figure 4.
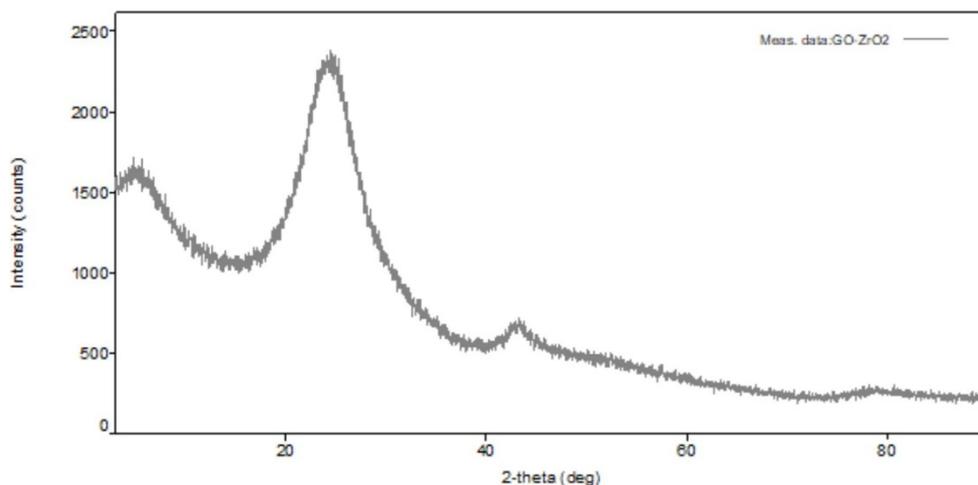
Figure 4. XRD diffractogram of composite ZrO_2/GO.

Textural properties

Textural properties of any material are significant in order to describe important material properties such as strength, chemical reactivity, deformation behavior, and many others. In the following Table 1, textural parameters of N_2 physisorption of both materials GO and ZrO_2/GO are given.

Table 1. Textural parameters of N_2 physisorption of GO and ZrO_2/GO samples

N$_2$ physisorption at 77 K		GO	ZrO$_2$/GO
Pore volume (Gurvich) at p/p$_0$, cm^{3}g^{-1}	0.999	0.136	0.223
	0.98	0.018	0.051
	0.95	0.010	0.042
(B.E.T.) 2 parameters	C	133.0	129.0
	S, m^{2}g^{-1}	6.6	51.3
Mesopores (B.J.H.) Desorption, Standard isotherm: Lecloux for corresponding C value from literature [28]	D$_{median}$, nm	18.5	7.6
	D$_{max}$, nm	3.6	3.6
	V$_{meso}$, cm^{3}g^{-1}	0.012	0.037
Mesopores (Dollim and Heal) Adsorption, Standard isotherm: Lecloux for corresponding C value from literature [28]	D$_{median}$, nm	22.7	9.6
	D$_{max}$, nm	2.4	2.0
	V$_{meso}$, cm^{3}g^{-1}	0.010	0.029

N$_2$ physisorption at 77 K		GO	ZrO$_2$/GO
Micropores (Horvath and Kawazoe), with potential function: Nitrogen on graphite at 77.3 K from literature [29]	D$_{max}$, nm	1.75	0.75
	V$_{meso}$, cm^{3}g^{-1}	0.003	0.021(5)
Micropore volume (Dubinin and Raduskevich)	cm^{3}g^{-1}	0.002(5)	0.180
Surface Area (Kaganer)	m^{2}g^{-1}	7.1	50.4
t-Plot Lecloux 300 > C(Bet) > 100 (Lippens and de Boer) from literature [28]	Total surface area, m^{2}g^{-1}	6.5	48.4
	Micropore volume, cm^{3}g^{-1}	0.002	0.26(5)
	Mesopores surface, m^{2}g^{-1}	3.8	7.9

N$_2$ adsorption onto GO and **ZrO$_2$/GO** gives type II isotherms, which means that our samples are nonporous or macroporous materials. These isotherms are represented in the Figure 5.
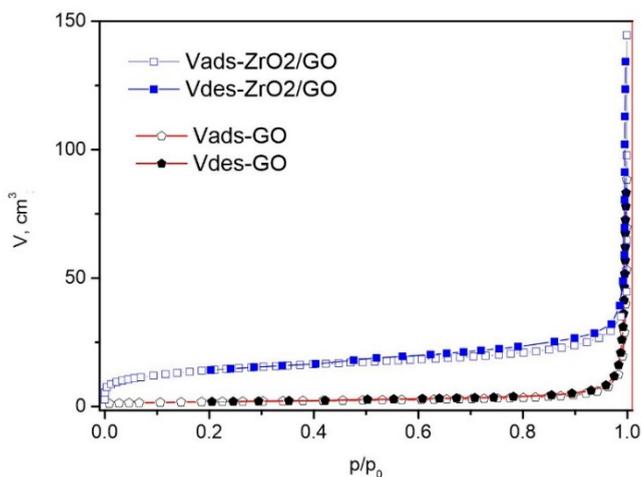
Figure 5. N$_2$ adsorption isotherms of GO and ZrO$_2$/GO samples.

The characteristic shape is the result of nonrestricted monolayer-multilayer adsorption up to high p/p$_0$. Gradual curvature or more precisely less distinctive knee on the curve is an indication of a significant amount of overlap monolayer coverage and the onset of multilayer adsorption. Type H3 hysteresis is observed for both samples which is characteristic of non-rigid aggregates of plate-like particles or systems with macropores that are not completely filed with pore condensate [30].
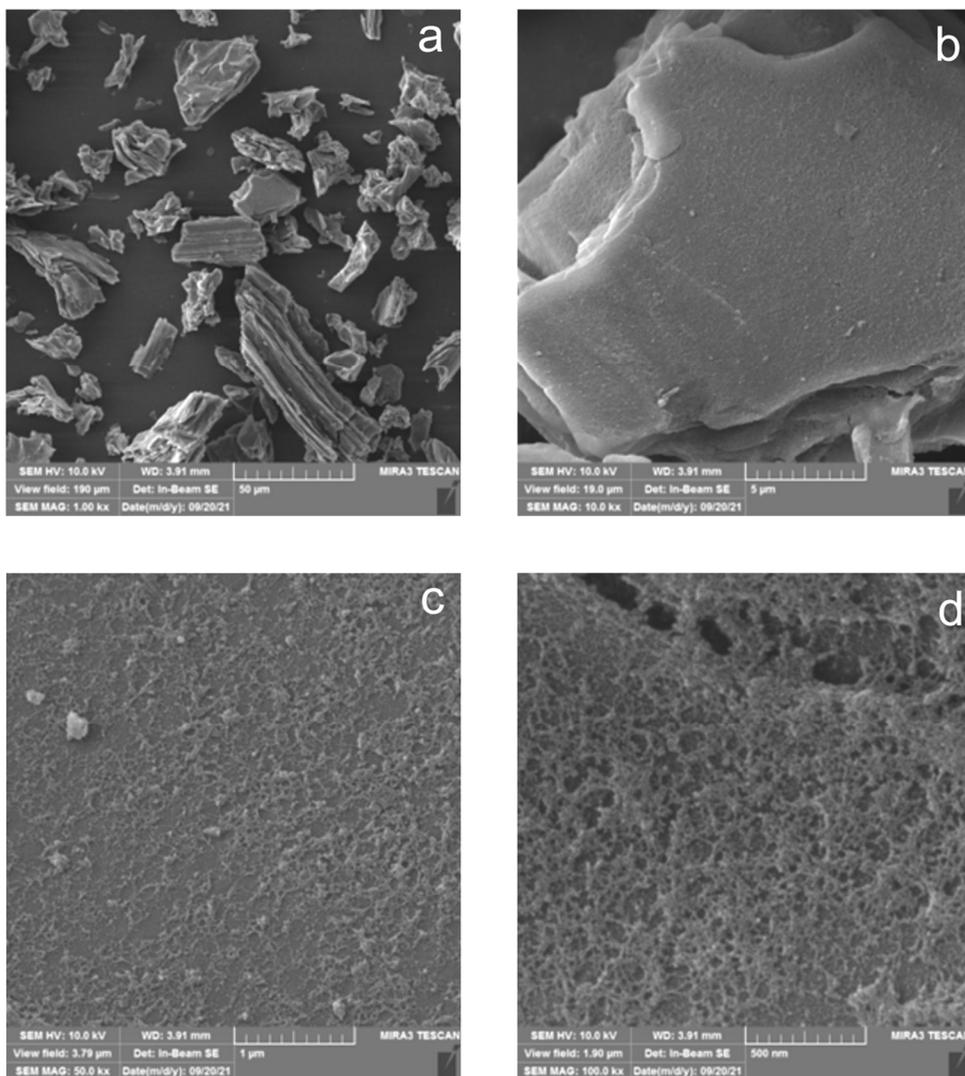
Figure 6. SEM micrograms of pure GO sample (a, b) and ZrO$_2$/GO sample (c, d).

SEM images confirm that the material has a plate-like structure of GO particles with a uniform coating of ZrO$_2$ onto GO particles. GO particles have a layered structure with dimensions around 20 nm. ZrO$_2$ coating has a reticular feature. The coating is uniform with submicrometer dimensions of particles. These SEM pictures are represented in Figure 6.

Sorption

Sorption experiments were conducted in batch mode with 50 cm^3 of dye solution and 50 mg of materials, and stirred on a magnetic stirrer in the dark. Aliquots are taken at specified periods of time and the concentration of dye was determined by a UV-Vis spectrophotometer. For sorption experiments two dyes are chosen, Methylene blue as a cationic dye, and Reactive blue 19 as anionic.

Effect of contact time - The initial concentration of MB was 100 mg dm^{-3} and for RB 19 was 10 mg dm^{-3}. Both materials GO and ZrO_2/GO are tested. Results for GO are shown in Table 2, while results for composite ZrO_2/GO are shown in Table 3. All results are expressed as the removal of dye as a function of time.

Table 2. Removal of MB and RB 19 dyes by pure GO.

GO	Dye removal, in percentage %	
Time, h	MB	RB 19
0.00	0.00	0.00
0.25	40.65	6.73
0.50	42.87	7.06
0.75	46.49	7.17
1.00	50.28	7.85
2.00	64.77	8.41
3.00	68.01	8.52
4.00	74.23	9.30
6.00	81.31	10.31

Table 3. Removal of MB and RB 19 dyes by composite ZrO_2/GO.

ZrO_2/GO	Dye removal, in percentage %	
Time, h	MB	RB 19
0.00	0.00	0.00
0.25	11.23	36.55
0.50	13.77	44.83
0.75	14.50	45.05
1.00	14.59	46.26
2.00	19.12	47.48
3.00	21.38	48.25
4.00	22.83	49.69
6.00	28.81	52.12

From the results shown in Tables 2 and 3, we can see that unmodified GO shown better sorption characteristics for cationic dye MB, while modified material ZrO_2/GO shown much better removal for anionic dye RB 19.

For all four experiments can be seen that the removal of dyes is more efficient and very fast in the first 30 minutes. After that period of time, free active sites on the material surface become occupied and the removal rate started to slow down and a near-equilibrium state is obtained after 3 hours.

Effect of initial concentration of dyes – These tests were conducted for both dyes. For MB dye initial concentrations were 10, 50, 100, and 200 mg dm^{-3}, and 1, 2.5, 5, and 10 mg dm^{-3} were concentrations of RB 19 dye. 50 cm^3 of dye solution and 50 mg of the composite were stirred in the dark for 2 hours. After 2 hours, solutions were centrifuged to separate composites from suspension. The solution was analyzed on a UV-Vis spectrophotometer to determine the final concentration. Results for GO are shown in Table 4, while results for composite ZrO$_2$/GO are shown in Table 5.

Table 4. Effect of initial concentration of MB and RB 19 dyes on pure GO.

GO					
MB			**RB 19**		
Initial concentration, mg dm^{-3}	Dye removal, %	Sorption capacity, mg g^{-1}	Initial concentration, mg dm^{-3}	Dye removal, %	Sorption capacity, mg g^{-1}
10.0	100.00	9.22	1.0	18.77	0.20
50.0	98.21	48.06	2.5	16.53	0.47
100.0	64.77	65.11	5.0	13.44	0.76
200.0	45.09	86.28	10.0	8.40	0.89

Table 5. Effect of initial concentration of MB and RB 19 dyes on composite ZrO$_2$/GO.

ZrO$_2$/GO					
MB			**RB 19**		
Initial concentration, mg dm^{-3}	Dye removal, %	Sorption capacity, mg g^{-1}	Initial concentration, mg dm^{-3}	Dye removal, %	Sorption capacity, mg g^{-1}
10.0	71.42	5.50	1.0	100.00	0.97
50.0	26.30	4.31	2.5	86.85	2.13
100.0	20.14	9.77	5.0	62.19	3.07
200.0	13.49	11.54	10.0	46.26	4.89

Sorption capacity increased for both materials and both dyes with increasing initial dye concentration. This can be explained by the increase of driving force [31]. Also can be observed that removal of MB dye is more effective with pure GO, while composite ZrO$_2$/GO is more effective in RB 19 dye removal.

Effect of sorbent dose – These tests were also conducted for both materials. Sorbent doses for both GO and ZrO_2/GO materials were 10, 20, 50, and 100 mg. 50 cm^3 of dye solution and an appropriate dose of sorbent were stirred in the dark for 2 hours. After 2 hours, solutions were centrifuged to separate composites from suspension. The solution was analyzed on a UV-Vis spectrophotometer to determine the final concentration. Results for GO are shown in Table 6, while results for composite ZrO_2/GO are shown in Table 7.

Table 6. Effect of sorbent dose of GO on final dye concentration.

GO					
MB			RB 19		
Sorbent dose, mg	Dye removal, %	Sorption capacity, mg g^{-1}	Sorbent dose, mg	Dye removal, %	Sorption capacity, mg g^{-1}
10.0	2.96	12.29	10.0	3.43	0.89
20.0	31.04	66.79	20.0	6.18	0.83
50.0	60.57	54.40	50.0	11.47	0.63
100.0	100.00	44.82	100.0	19.08	0.53

Table 7. Effect of sorbent dose of ZrO_2/GO on final dye concentration.

ZrO_2/GO					
MB			RB 19		
Sorbent dose, mg	Dye removal, %	Sorption capacity, mg g^{-1}	Sorbent dose, mg	Dye removal, %	Sorption capacity, mg g^{-1}
10.0	20.76	9.30	10.0	14.80	0.73
20.0	33.67	7.62	20.0	54.72	1.37
50.0	71.42	5.50	50.0	100.00	1.03
100.0	100.00	4.64	100.0	30.76	0.16

When the effect of sorption dose is observed, for both materials can be seen that removal increases with the increase of sorbent dose. The exception is the removal of RB 19 with ZrO_2/GO, where 100% removal is achieved with 50 mg of sorbent, and about 30% with 100 mg. Sorption capacity decreases for removal of RB 19 with GO, and MB with ZrO_2/GO, while we have an initial increase and further decrease for removal of MB with GO and RB 19 with ZrO_2/GO. Amount adsorbent per unit mass of the adsorbent decrease due to adsorption sites remaining unsaturated during the adsorption reaction [32,33].

Photocatalysis

The photocatalytic ability of presented materials was studied using the degradation of organic dyes Methylene blue and Reactive blue 19 using the ZrO_2/GO composite. Photocatalytic experiments were conducted under UV light with maximum emission at 254 nm. In all experiments irradiation of six lamps, 28 W each were applied. Effect of time, initial dye concentration, and composite mass were investigated.

Effect of irradiation time - Tests were conducted in a UV reactor during the two hour period of irradiation. The experimental setup was that 50 cm^3 of dye solution (initial concentration for RB 19 was 10 mg dm^{-3} and for MB 100 mg dm^{-3}) was stirred on a magnetic stirrer in an opened glass beaker with 50 mg of composite ZrO_2/GO (1 g dm^{-3}). Aliquots were taken at the specified time, centrifuged, and concentration (absorbance) was calculated from absorbance determined by UV-Vis spectrophotometer using equations given in experimental part. Results are shown as degradation rate as a function of time and represented in Figure 7 for MB and Figure 8 for RB 19 dye.
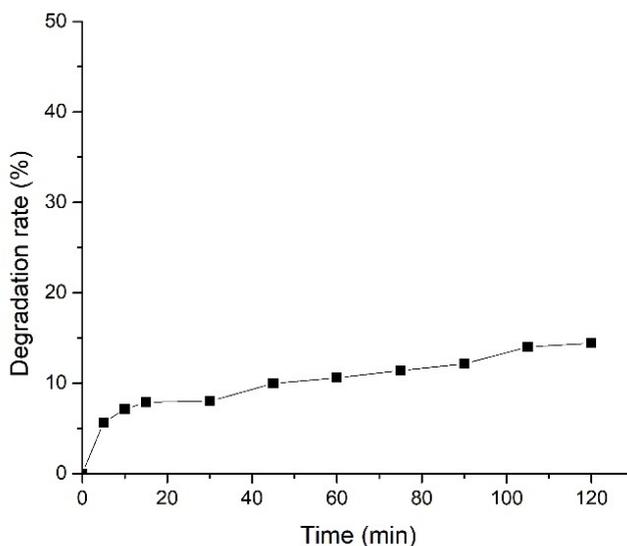
**Figure 7.** Effect of irradiation time on degradation of MB dye.
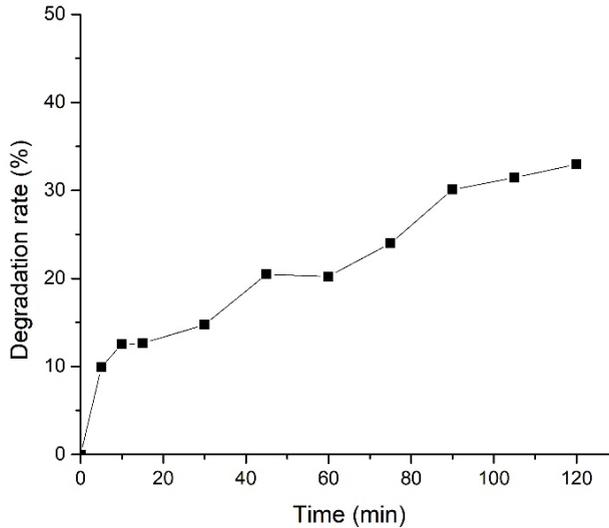
**Figure 8.** Effect of irradiation time on degradation of RB 19 dye.

From Figures 7 and 8 can be seen that a better degradation rate is achieved for RB 19 dye (about 33%) while the degradation rate of MB is relatively low (only 14%). For both dyes, the increase of degradation rate during the time is slow but constant, so we can suggest that equilibrium is achieved after 90 minutes of irradiation.

Effect of initial concentration of dyes – This effect was conducted for both dyes. For MB dye initial concentrations were 10, 50, 100, and 200 mg dm^{-3}, and 1, 2.5, 5, and 10 mg dm^{-3} were concentrations of RB 19 dye. Tests were conducted in a UV reactor during the two hour period of irradiation. Results are shown as degradation rate as a function of time and represented in Figure 9 for RB 19 and Figure 10 for MB dye.

From Figure 9 can be seen that the degradation rate of RB 19 dye is highly dependent on initial dye concentration. Results show that degradation rate increase from 19% for 5 mg dm^{-3} up to 100% for 1 mg dm^{-3}. Also, as the initial concentration increases degradation process became faster, and for the lowest initial concentration, after 75 min we achieved total degradation. For other concentrations, 90 or more minutes were needed to achieve the maximum degradation rate.
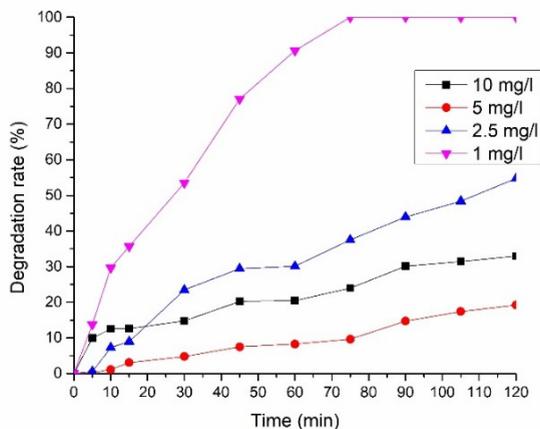
Figure 9. Effect of initial concentration of RB 19 dye on degradation.
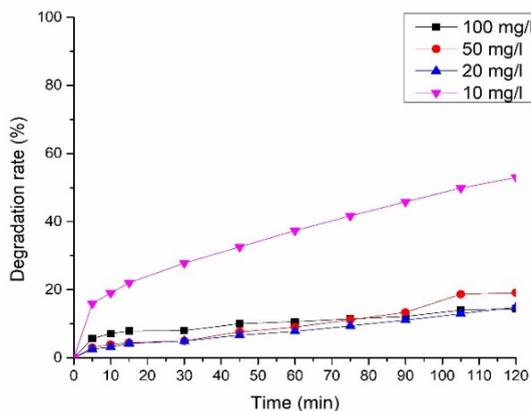
Figure 10. Effect of initial concentration of MB dye on degradation.

Degradation of MB dye is also dependent on the initial dye concentration but is not so obvious as in RB 19 dye case. In the case of MB dye, we have almost the same degradation rate for concentrations between 20 and 100 mg dm^{-3} (14% to 19%). Also, equilibrium is reached after 45 minutes for all samples. The notable increase in degradation rate is achieved for MB concentration 10 mg dm^{-3} without reaching equilibrium.

Effect of amount of composite – Next two figures show the dependence of the degradation rate of dyes as a function of the amount of composite in the system, where we have tested four different amounts (10, 20, 50, and 100 mg). Tests were carried out with an initial concentration of MB 10 mg dm^{-3} and RB 19 1 mg dm^{-3}. 50 cm^3 of dye solution was stirred in a UV reactor in an open glass beaker with the appropriate amount of ZrO$_2$/GO composite. Results are shown as degradation rate as a function of time and represented in Figure 11 for MB and Figure 12 for RB 19 dye.
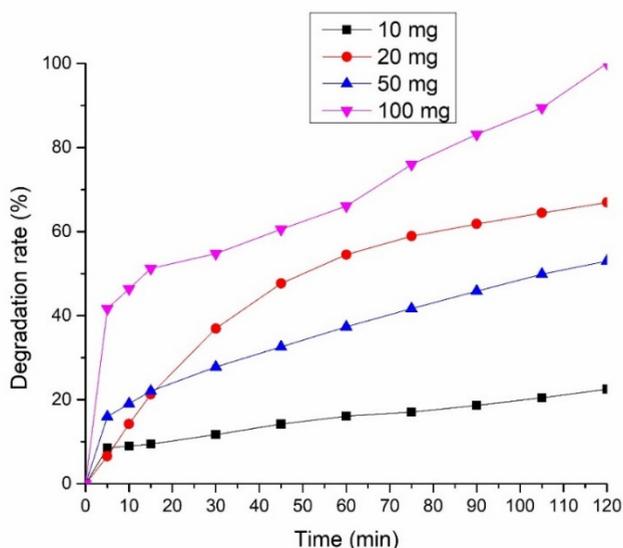
Figure 11. Effect of amount of ZrO$_2$/GO composite on degradation of MB dye.

From Figure 11 can be seen that the degradation rate of MB dye increases as the amount of composite in the system increase. That is quite expected because with increasing amounts of composite, there are more active sites in the system, so more photons can be involved in the photocatalytic process.

An increase in the amount of composite leads to an increase in the degradation rate of RB 19 dye as we can see from Figure 12. As mentioned above, more composite in the system means more active sites, thus the photocatalytic process is more effective. In the case of RB 19 dye, we have total degradation with amounts of composite over 20 mg and with an increase in mass, we have faster total degradation.
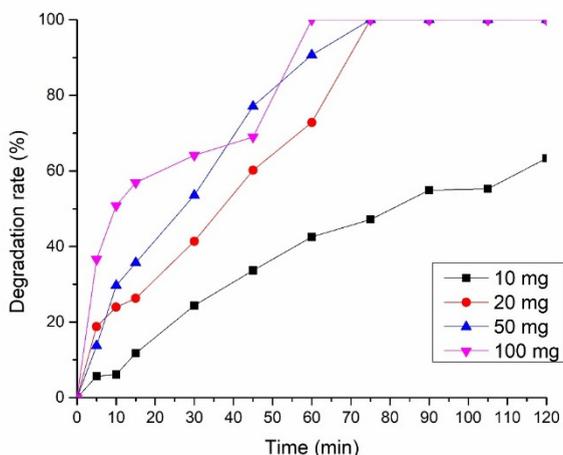
Figure 12. Effect of amount of ZrO_2/GO composite on degradation of RB 19 dye.

CONCLUSIONS

In this paper, we presented the first results of a novel composite and its applications as sorbent and photocatalyst. Results are promising especially for photocatalysis because neither pure zirconia or pure graphene oxide is not photocatalytic active. With this method of synthesis of ZrO_2/GO composite we have obtained possible good photocatalytic material for a wide range of usage. We believe that this paper is only the beginning of new wider research for obtaining more effective and low-cost materials for photocatalytic applications.

EXPERIMENTAL SECTION

Reagents and chemicals

All used chemicals, sodium-nitrate (Centrohem), sulfuric acid (Zorka Pharma), potassium-permanganate (Zdravlje), hydrochloric acid (Zorka Pharma), ethanol (Zorka Pharma), zirconium-isopropoxide (Acros Organics), 2-propanol (Sigma Aldrich), ammonium hydroxide (NRK engineering), Methylene Blue (Merck), Reactive Blue 19 (Merck) were analytical grade and used without further purification. Graphite was commercial grade from Trayal factory with unknown origin. Deionized water was used in all experiments.

Preparation of materials

Graphene oxide preparation - Graphene oxide was synthesized via the modified Hummers-Offeman method [20], where we have the oxidation of graphite with a strong oxidizing agent to exfoliate graphite. The first step was mixing 5.0 g of natural graphite powder of fine grade (150 μm), 2.5 g of sodium nitrate, and 115.0 cm^{-3} of concentrated sulfuric acid in an ice bath, in order to cool the mixture to 0°C. After mixing this suspension for 30 minutes, 15.0 g of potassium permanganate was added in small portions, where the temperature in the reactor needs to be lower than 20°C. After this step, the reactor was heated to 35±3°C and kept at this temperature for the next 30 minutes. As the reaction progressed, the suspension got brownish-grey color and became pasty. In the next step after these additional 30 minutes period, 230.0 cm^{-3} of water was slowly stirred into the paste to prevent violent effervescence, and as a result, the temperature increased to 95-98°C, and this diluted brown suspension was mixed at this temperature for 15 minutes. After 15 minutes, 5.0 cm^{-3} of hydrogen peroxide and additional water (500.0 cm^{-3}) were added to reduce the residual permanganate and manganese dioxide to colorless soluble manganese sulfate and this leads to the bright yellow color of suspension. The last step was filtration of warm suspension and washing of the filter cake with distilled water, 30% hydrochloric acid, and ethanol (amount of each was 150.0 cm^{-3}). The dry product was obtained by centrifugation and was dried at 60°C for 24 hours.

ZrO$_2$/GO preparation - Zirconia-graphene oxide-based composites were synthesized using the modified sol-gel method, where as a precursor zirconia isopropoxide is used. In the first step of the synthesis, 1.6 cm^{-3} of zirconium isopropoxide was dissolved in 10.0 cm^{-3} of 2-propanol under inert conditions and added 2.0 g of previously synthesized graphene oxide. After that, the second solution (mixture of 20.0 cm^{-3} of water and 20.0 cm^{-3} of 2-propanol) was added drop by drop under vigorous stirring for 1 hour. After one hour of stirring, the pH of the mixture was adjusted to 9.5 by a mixture of NH_3 and H_2O in a volume ratio of 1:3. After that, the mixture was heated with a reflux condensator at 60°C for 3 hours. The last step was filtration of the wet gel and washing of the filter cake with distilled water and 2-propanol (amount of each was 100.0 cm^{-3}). The dry product was dried at 60°C for 24 hours and after that, 3 more hours at 120°C.

Characterization

X-ray diffraction (XRD) analyses were performed using the instrument Rigaku MiniFlex 600 with D/teXUltra 250 high-speed detector and Cu-anode.

Parameters of measurements were angle range 3-90°, step 0.02°, scanning speed 10°/min. The anode voltage was 40 kV and the current 15 mA. Identification was done using PDXL2 Version 2.4.2.0 software and obtained diffractograms were compared to the COD database.

Surface area and pore size distribution were determined by nitrogen adsorption-desorption isotherms. Measurements were done on Sorptomatic 1990 Thermo Finnigan automatic system by physisorption of nitrogen at -196°C. All samples were degassed before measurements at 130°C for 3 h. Specific surface area and pore size distribution were calculated by the BET method using ADO 5.13 Thermo Electron software.

FT-IR analyses were done using MB-100 infrared spectrometer (Bomem Hartman & Braun, Canada).

Morphology of composites was examined by Quanta 200 Scanning Electron Microscope (FEI, Hillsboro, Oregon, USA).

Sorption tests

Sorption tests were conducted in dark to avoid competition and the synergistic effect of sorption and photocatalysis. Cationic dye Methylene blue and anionic Reactive blue 19 dye were used in experiments. All experiments were done in batch mode, 50 cm^3 of dye solution in an Erlenmeyer flask covered with aluminum foil, and an adequate mass of composite was stirred on a magnetic stirrer for a defined period. Samples were collected at the specified time, centrifuged (Hermle Z207 A) for 15 min at 5000 r/min, and tested by UV-Vis spectrophotometer Shimadzu UV-Vis 1650 PC (Shimadzu, Japan). Effects of treatment time, initial dye concentration, and composite mass were investigated. For calculating concentration from absorbance, following equations from calibration curves are used:

$$C = 0.0843 * A + 0.0103 \, ; R^2 = 0.997$$

for RB 19, and:

$$C = 0.1829 * A + 0.0443 \, ; R^2 = 0.998$$

for MB.

Dye removal was calculated using the following equation:

$$R = \frac{C_0 - C_t}{C_0} * 100\%$$

Sorption capacity was calculated using formula:

$$Q = \frac{C_0 - C_t}{m_s} * V$$

In these equations, C is for concentration, R is removal, C_0 for initial concentration, C_t for concentration after time t, A is for absorbance, m_s is for mass of sorbent, and V is volume of solution.

Photocatalytic tests

Photocatalytic tests were performed in a UV reactor with 6 low-pressure Hg lamps (28 W) with maximum emission at 254 nm. Before all photocatalytic tests, the suspension of composite and color solution was stirred in the dark for 24 hours to obtain total adsorption-desorption equilibrium to avoid competition with the photocatalytic degradation process. Cationic dye Methylene blue and anionic Reactive blue 19 dye were used in experiments. Samples were collected at a specified time and centrifuged (Hermle Z207 A) for 15 min at 5000 r/min. The concentrations of dyes were determined by the UV-Vis spectrophotometer Shimadzu UV-Vis 1650 PC (Shimadzu, Japan). For calculating concentration from absorbance, following equations from calibration curves are used:

$$C = 0.0843 * A + 0.0103 \,; R^2 = 0.997$$

for RB 19, and:

$$C = 0.1829 * A + 0.0443 \,; R^2 = 0.998$$

for MB.

Degradation rate was calculated using:

$$D = \frac{C_0 - C_t}{C_0} * 100\%$$

In these equations, C is for concentration, Degradation rate is removal, C_0 for initial concentration, C_t for concentration after time t, A is for absorbance.

ACKNOWLEDGMENTS

REFERENCES

1. B. Lellis; C. Z. Fávaro-Polonio; J. A. Pamphile; J. C. Polonio; *Biotechnol. Res. Innov.,* **2019**, *3,* 275-290.
2. S. Y. Mak; D. H. Chen; *Dyes Pigm.*, **2004**, *61*, 93-98.
3. M. Rafatullah; O. Sulaiman; R. Hashim; A. Ahmad; *J. Hazard. Mater.*, **2010**, *177*, 70-80.
4. D. Ghosh; K. G. Bhattacharyya; *Appl. Clay Sci.*, **2002**, *20*, 295-300.
5. N. K. Nga; N. T. T. Chau; P. H. Viet; *J. Sci.: Adv. Mater. Dev.*, **2020**, *5*, 65-72.
6. A. H. Jawad; A. S. Abdulhameed; N. N. Abd Malek; Z. A. Alothman; *Int. J. Biol. Macromol.*, **2020**, *164*, 4218-4230.
7. S. T. Yang; S. Chen; Y. Chang; A. Cao; Y. Liu; H. Wang; *J. Colloid Interface Sci.*, **2011**, *359*, 24-29.
8. B. Manu; S. Chaudhari; *Bioresour. Technol.*, **2002**, *82*, 225-231.
9. M. Inagaki; T. Imai; T. Yoshikawa; B. Tryba; *Appl. Catal. B: Environ.*, **2004**, *51*, 247-254.
10. Y. Min; K. Zhang; W. Zhao; F. Zheng; Y. Chen; Y. Zhang; *Chem. Eng. J.*, **2012**, *193*, 203-210.
11. N. Zaghbani; A. Hafiane; M. Dhahbi; *Sep. Purif. Technol.*, **2007**, *55*, 117-124.
12. A. Dąbrowski; *Adv. Colloid Interface Sci.*, **2001**, *93*, 135-224.
13. G. Crini; *Bioresour. Technol.*, **2006**, *97*, 1061-1085.
14. K. Krishnamoorthy; R. Mohan; S. J. Kim; *Appl. Phys. Lett.*, **2011**, *98*, 244101.
15. M. N. Chong; B. Jin; C. W. Chow; C. Saint; *Water Res.*, **2010**, *44*, 2997-3027.
16. A. T. Smith; A. M. LaChance; S. Zeng, B. Liu; L. Sun; *Nano Materials Science*, **2019**, *1*, 31-47.
17. C. K. Chua; M. Pumera; *Chem. Soc. Rev.*, **2014**, *43*, 291-312.
18. Z. Wang; J. Liu; W. Wang; H. Chen; Z. Liu; Q. Yu; H. Zeng; L. Sun; *Chem. Commun.*, **2013**, *49*, 10835-10837.
19. X. Y. Wang; A. Narita; K. Müllen; *Nat. Rev. Chem.*, **2017**, *2*, 1-10.
20. W. S. Hummers Jr; R. E. Offeman; *J. Am. Chem. Soc.*, **1958**, *80*, 1339-1339.
21. L. C. Pop; G. Barta; L. C. Cotet; K. Magyari; M. Baia; L. B. Tudoran; R. Ungur; D. Vodnar; L. Baia; V. Danciu; *Stud. Univ. Babes-Bolyai Chem.*, **2022**, *67*, 281-296.
22. L. Wang; J. Ding; Y. Chai; Q. Liu; J. Ren; X. Liu; W. L. Dai; *Dalton Trans.*, **2015**, *44*, 11223-11234.
23. P. S. Chauhan; R. Kant; A. Rai; A. Gupta; S. Bhattacharya; *Mater. Sci. Semicond. Process.*, **2019**, *89*, 6-17.
24. X. Luo; C. Wang; L. Wang; F. Deng; S. Luo; X. Tu; C: Au; *Chem. Eng. J.*, **2013**, *220*, 98-106.
25. H. Di; Z. Yu; Y. Ma; C. Zhang; F. Li; L. Lv; Y. Pan; H. Shi; Y. He; *J. Taiwan Inst. Chem. Eng.*, **2016**, *67*, 511-520.
26. G.I. Titelman; V. Gelman; S. Bron; R.L. Khalfin; Y. Cohen; H. Bianco-Peled; *Carbon*, **2005**, *43*, 641-649.

27. J. Lai; S. Zhou; X. Liu; Y. Yang; J. Lei; Q. Xu; D. Yin; *Catal. Lett.*, **2019**, *149*, 2749-2757.
28. A. Lecloux; J. P. Pirard; *J. Colloid Interface Sci.*, **1979**, *70*, 265-281.
29. G. Horvath; K. Kawazoe; *J. Chem. Eng. Japan*, **1983**, *16*, 470-475.
30. M. Thommes; K. Kaneko; A. V. Neimark; J. P. Olivier; F. Rodriguey-Reinoso; J. Rouquerol; K. S. W. Sing; *Pure Appl. Chem.*, **2015**, *87*, 1051-1069.
31. M. Kostić; S. Najdanović; N. Velinov; M. Radović Vučić; M. Petrović; J. Mitrović; A. Bojić; *Environ. Technol. Innov.*, **2022**, *26*, 102358.
32. Y. Bulut; H. Aydin; *Desalination*, **2006**, *194*, 259-267.
33. C. Raji; T. S. Anirudhan; *Indian J. Chem. Technol.*, **1997**, *4*, 157-162.